

Phase maps of microelectromechanical switches in the presence of electrostatic and Casimir forces

G. Palasantzas* and J. Th. M. DeHosson

Department of Applied Physics, Materials Science Center, University of Groningen, Nijenborgh 4, 9747 AG Groningen, The Netherlands

(Received 14 July 2005; published 29 September 2005)

In this paper we explore the influence of self-affine roughness on the phase maps for switches used in nano- and/or microelectromechanical devices in the presence of the Casimir and electrostatic forces. It is shown that the phase map depends significantly on the characteristic roughness parameters (roughness amplitude w , correlation length ξ , and roughness exponent H). The phase maps depend sensitively on the short wavelength roughness as it is described by the roughness exponent H . For conditions close to instability the precise knowledge of the latter is highly important since minor variations of $H(\pm 0.05)$ cause the system to become unstable that if both electrostatic and Casimir forces are acting.

DOI: 10.1103/PhysRevB.72.121409

PACS number(s): 68.55.-a, 68.60.Bs, 87.50.Rr, 85.70.Kh

The design of micro- and/or nanoelectromechanical (MEMS/NEMS) applications such as nanotweezers, nanoscale actuators, etc., requires, in many cases, the use of microswitches.¹⁻¹⁰ A typical switch is constructed from two conducting electrodes having one usually fixed and the other one moving but suspended by the use of a mechanical spring. With the application of a voltage difference between the two electrodes, the movable electrode moves towards the ground electrode because of the electrostatic force. At a certain voltage, the moving electrode becomes unstable and collapses or pulls in to the ground plate.³ A two-degrees of freedom pull-in model is presented in Ref. 4 for a direct calculation of the electrostatic actuators. Residual stress and the fringing-field effect have also been shown to have great influence on the behavior of rf switches and to strongly influence their failure characteristics.^{5,6}

The pull-in voltage when van der Waals forces are present between the plates was studied in Ref. 11 by ignoring its influence on the pull-in gap. However, in Ref. 12 the effect of the van der Waals force on the pull-in gap was investigated and an analytical expression of the pull-in gap and pull-in voltage based on a more general model was presented.¹² The dynamical behavior for nanoscale electrostatic actuators was studied by considering the effect of the van der Waals force in Ref. 13. In addition, the Casimir effect on the pull-in gap, pull-in voltage, and phase maps of NEMS switches was also studied in Ref. 10. An approximate expression of the pull-in gap with the Casimir force was presented by using the perturbation theory.¹⁴ Notably, the Casimir effect is a prediction of quantum electrodynamics that results from the perturbation of zero point vacuum fluctuations by conducting plates.¹⁶⁻¹⁸

Recently, the influence of the Casimir force was studied on the nonlinear behavior of nanoscale electrostatic actuators for the case of flat electrodes.¹⁵ It was also found that the phase maps show periodic orbits to exist around the Hopf point, and a homoclinic orbit to pass through an unstable saddle point.¹⁵ Up to now the previous studies did not consider the influence of plate roughness through the Casimir force and the electrostatic force on the phase maps. More-

over, in many cases the roughness of deposited metal layers (e.g., by sputtering, thermal evaporation, e -beam evaporation, etc.) is termed as self-affine¹⁹ and its influence will be considered here in significant detail in terms of analytic models for the power spectrum in Fourier space.

Furthermore, we consider here a parallel plate configuration with the electrostatic force and Casimir force pulling the plates together, while an opposing elastic restoring force (with mass-spring form) is present. The initial plate distance is d , the average flat plate surface area A_f , the plate spring constant k and its mass m , the voltage across the plates V , and ϵ_o the vacuum permittivity. The restoring and electrostatic forces for a plate separation $r(\leq d)$ are given by¹⁵

$$F_k = -k(d-r) \quad \text{and} \quad F_e \cong \frac{\epsilon_o A_r V^2}{2r^2}. \quad (1)$$

A_r is the surface area of a rough plate surface. Assuming single valued roughness fluctuations $h(R)$ of the in-plane position $R=(x,y)$ the Casimir energy is²⁰

$$E_{cr} \cong E_{cf} + \frac{1}{2} \left(\frac{\partial^2 E_{cf}}{\partial r^2} \right) \sum_{m=1}^2 \int \frac{d^2 q}{(2\pi)^2} P_m(q) \langle |h_m(q)|^2 \rangle, \quad (2)$$

with $E_{cf} = -(\pi^2 c / 720 r^3) A_f$, and $\langle |h_m(q)|^2 \rangle$ the roughness spectra ($\langle h_m \rangle = 0$). For $r > \lambda_p$ with λ_p the surface plasmon wavelength we have $P_m(q) = qr/3 (qr > 1)$.²⁰ Furthermore, Eq. (2) yields, assuming the same roughness for both plates,

$$F_{cr} = -\frac{dE_{cr}}{dr} \cong F_{cf} \left(1 + \frac{2C_r}{3r} \right), \quad (3)$$

$$C_r = \int_{Q_d}^{Q_c} q \langle |h_{m=1,2}(q)|^2 \rangle \frac{d^2 q}{(2\pi)^2},$$

with $Q_d = 2\pi/d$ and $Q_c = \pi/a_o$ where a_o is of the order of atomic dimensions.

If we set $u=r/d$, $M=m/kT^2$, $\tau=t/T$ (T a characteristic time), $\alpha = \pi^2 A_f / kd^5$, and $\beta = \epsilon_o A_f V^2 / kd^3$,¹⁵ the second law of Newton $m(d^2 r / dt^2) = (|F_k| - |F_e + F_{cr}|)$ that describes the plate motion takes the alternative form

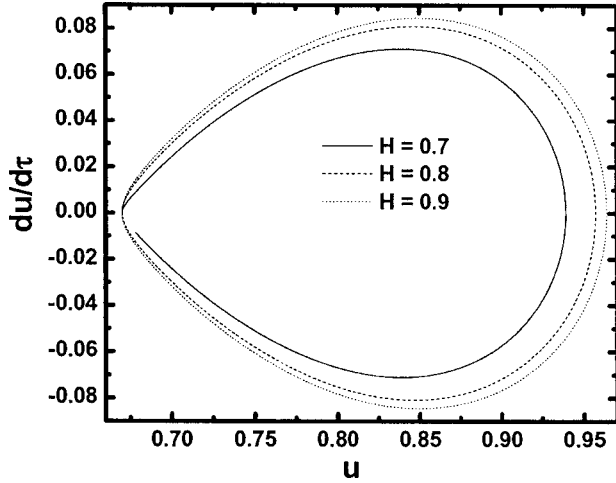


FIG. 1. Calculation of phase maps $du/d\tau$ vs u for $a_o=0.3$ nm, $M=1$, $d=200$ nm, $w=5$ nm, $\xi=200$ nm, $a=10$, $\beta=0.1$, and various consecutive values of the roughness exponent H as indicated.

$$M \frac{d^2u}{d\tau^2} = 1 - u - \frac{\beta R_r}{2u^2} - \frac{\alpha}{240u^4} \left(1 + \frac{2C_r}{3du} \right), \quad (4)$$

with meaningful solutions for $0 < u < 1$ and $A_r = A_f R_r$. Moreover, for Gaussian height distribution²¹ we have $R_r = \int_0^{+\infty} e^{-y} (1 + \rho_{rms}^2 y)^{1/2} dy$, where the average local surface slope $\rho_{rms} = [\langle |\nabla h|^2 \rangle]^{1/2}$ is given by $\rho_{rms} = [\int_0^{Q_c} q^2 \langle |h(q)|^2 \rangle d^2q / (2\pi)^2]^{1/2}$ (Ref. 22).

A wide variety of surfaces and interfaces that appear in films grown under nonequilibrium conditions possess the so-called self-affine roughness.¹⁹ In this case the roughness spectrum shows a power law scaling¹⁹ $\langle |h(q)|^2 \rangle \propto q^{-2-2H}$ if $q\xi \gg 1$ and $\langle |h(q)|^2 \rangle \propto \text{const}$ if $q\xi \ll 1$. This is satisfied by the analytic model $\langle |h(q)|^2 \rangle = [2\pi w^2 \xi^2 / (1 + aq^2 \xi^2)^{1+H}]^{23}$ with $a = \frac{1}{2} H [1 - (1 + aQ_c^2 \xi^2)^{-H}]$ ($0 < H < 1$), $a = \frac{1}{2} \ln(1 + aQ_c^2 \xi^2)$ ($H = 0$). $Q_c = \pi/a_o$ with a_o of the order of atomic dimensions. Small values of H (~ 0) characterize jagged or irregular surfaces; while large values H (~ 1) surfaces with smooth hills and valleys.¹⁹ For other models see also Refs. 24 and 25.

The calculations of the phase maps were performed with lower roughness cut-off $a_o=0.3$ nm, effective system mass $M=1$, and initial conditions $u=0.67$ and $du/d\tau=0$ (at $\tau=0$). Figure 1 shows calculations of phase maps ($du/d\tau$ vs u) for various roughness consecutive roughness exponents H . With decreasing roughness exponent H (or for a roughened surface at short wavelengths) the phase map is squeezed in size in a rather sensitive manner even for consecutive exponents. This is rather significant since under normal experimental conditions the roughness exponent H is determined with accuracy (e.g., by scanning probe microscopy, x-ray reflectivity, electron diffraction, etc.¹⁹) of approximately $\pm(0.05-0.1)$. Thus, the latter has significant implications on the accurate prediction of the phase maps for MEMS/NEMS switch systems and their stability.

For lower roughness exponents $H(<0.7)$ an instability develops that is due to the fact that the surface area term increases leading to larger effective parameters βR_r , approach-

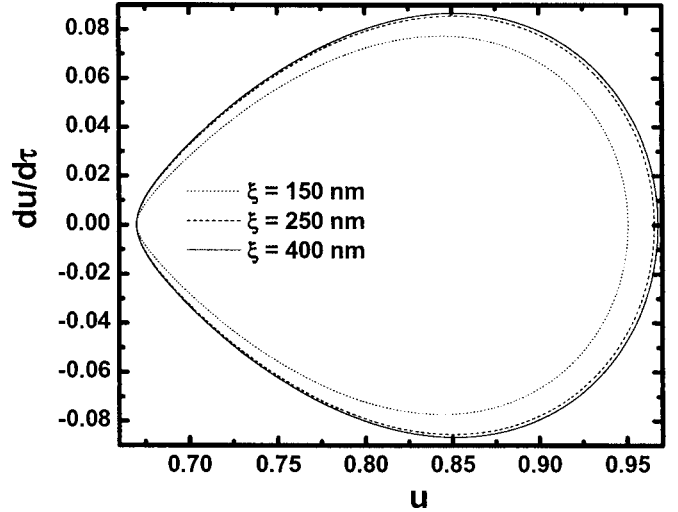


FIG. 2. Calculation of phase maps $du/d\tau$ vs u for $a_o=0.3$ nm, $M=1$, $d=200$ nm, $w=5$ nm, $a=10$, $\beta=0.1$, roughness exponent $H=0.9$, and correlation lengths ξ as indicated.

ing forbidden values that prevent stable behavior for $0 < u < 1$. In the weak roughness limit (or $\rho_{rms} < 1$), which is the case that Eq. (2) for the Casimir force applies, we have $R_r \approx 1 + \rho_{rms}^2/2$, which gives the correction to the parameter β , namely $\beta \rho_{rms}^2/2$. Notably in terms of the analytic model for $\langle |h(q)|^2 \rangle$ we have also the analytic form $\rho_{rms} = (w/\xi\sqrt{2a}) \{ [(1 + aQ_c^2 \xi^2)^{1-H} - 1]/(1-H) \} - 2a)^{1/2}$ (Ref. 22) and thus an analytic correction for β (indeed $\beta \leq 0.2$ for flat surfaces¹⁵) for any roughness exponent H .

Furthermore similar behavior develops with increasing the long wavelength roughness parameter w while decreasing the lateral correlation length ξ as shown in Figs. 2 and 3. In all cases surface roughening (at short and/or long lateral roughness wavelengths) leads to squeezed phase maps. Clearly if we compare Figs. 1–3, the highest sensitivity towards unstable behavior arises from the roughness parameters w and H , with the roughness exponent H having the

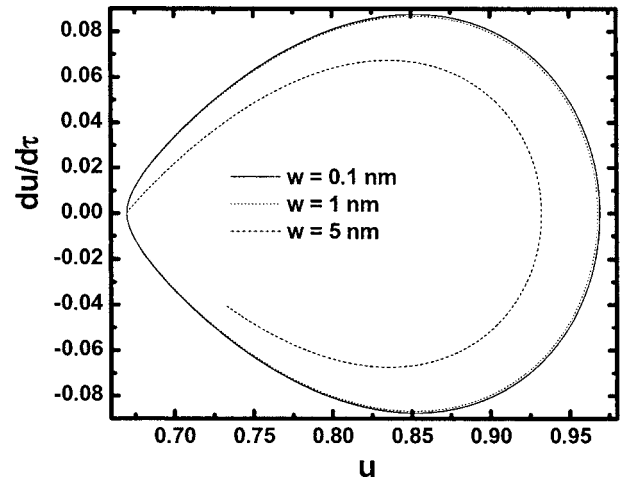


FIG. 3. Calculation of phase maps $du/d\tau$ vs u for $a_o=0.3$ nm, $M=1$, $d=200$ nm, $\xi=100$ nm, $a=10$, $\beta=0.1$, roughness exponent $H=0.8$, and various roughness amplitudes w as indicated.

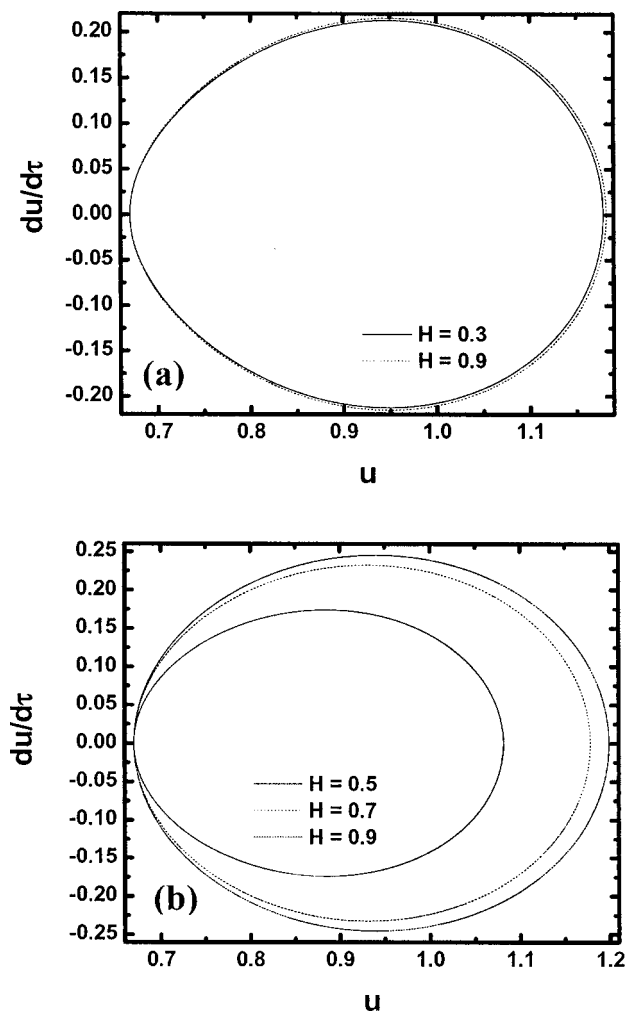


FIG. 4. (a) Calculation of phase maps $du/d\tau$ vs u for $a_0 = 0.3$ nm, $M=1$, $d=200$ nm, $\xi=100$ nm, $a=10$, $\beta=0$, $w=5$ nm, and various roughness exponent H as indicated. (b) Calculation of phase maps $du/d\tau$ vs u for $a_0=0.3$ nm, $M=1$, $d=200$ nm, $\xi=100$ nm, $a=0$, $\beta=0.1$, $w=5$ nm, and various roughness exponent H as indicated.

most sensitive contribution. In this case a change of the latter even with the limits of its measurement can lead to significant changes of the phase maps and to unstable behavior. On the other hand, the effect of the roughness amplitude w becomes significant when the latter changes by more than an order of magnitude towards the strong roughness limit that is dictated by local surface slopes $\rho_{rms} > 1$.

Clearly if we compare Figs. 1–3 where both attractive (Casimir and electrostatic) forces contribute with Figs. 4(a) and 4(b), the presence of the Casimir force, although weak, can strongly alter the phase maps of the device. Despite the fact that the major influence of the surface roughness comes through the electrostatic term, the presence of the Casimir force modifies the system motion and confines to permissible values $u < 1$. Clearly the influence of the roughness exponent H plays a prominent role as Figs. 1 and 4 clearly shown. Therefore, in devices where metallic surface layers are deposited in between moving surfaces, accurate roughness characterization is required in order to gauge properly the morphology influence on device performance.

Finally, we should mention that in this paper the Casimir force and energy are calculated assuming perfect conductors. However, the Casimir force and energy depend on the dielectric properties of the materials in a complicated manner.²⁶ On the other hand, in NEMS and MEMS, real materials are involved and dielectric properties are important for the Casimir force. If, however, we restrict ourselves to the influence of roughness, the assumption of perfect conductors is valid. Moreover, we should note that the perturbative calculations of the Casimir force always lead to a roughness correction that is larger than the result obtained within the proximity force approximation^{20,27} (PFA). In the present paper we consider our calculations for the case of perfectly reflecting mirrors assuming plate separations $r > \lambda_p$,²⁰ while for shorter distances the effect of finite conductivity should be considered.²⁷

In conclusion, phase maps of switches with self-affine rough plate surfaces where both electrostatic and Casimir forces are present appear to depend sensitively on the short wavelength roughness as it is described by the roughness exponent H . For situations close to instability the precise determination of the latter is highly important. We should point out that although the major influence of the surface roughness comes through the electrostatic term, the presence of the Casimir force modifies the system motion and makes more sensitive its dependence on the characteristic roughness parameters. Therefore, proper surface roughness measurements are necessary to characterize the morphology (e.g., by x-ray scattering techniques, electron diffraction, scanning probe microscopy,^{19,23–25} etc.) at all relevant roughness wavelengths in order to gauge its influence on the Casimir and electrostatic forces.

The authors would like to thank Professor A. A. Maradudin for discussions on the Casimir effect.

*Corresponding author. Electronic address: g.palasantzas@rug.nl

¹P. Kim and C. M. Lieber, *Science* **286**, 2148 (1999).

²S. Akita *et al.*, *Appl. Phys. Lett.* **79**, 1691 (2001).

³P. M. Osterberg, Ph.D. dissertation, MIT, 1995.

⁴O. Bochobza-Degani and Y. Nemirowsky, *Sens. Actuators, A* **97–98**, 569 (2002).

⁵O. Bochobza-Degani, E. Socher, and Y. Nemirowsky, *Sens. Ac-*

tuators, A **97**, 563 (2002).

⁶L. X. Zhang, J. W. Zhang, Y.-P. Zhao, and T. X. Yu, *Int. J. Non-linear Sci. Numer. Simul.* **3**, 353 (2002).

⁷L. X. Zhang and Y.-P. Zhao, *Microsyst. Technol.* **9**, 420 (2003).

⁸L. J. Hornbeck, U.S. Patent No. 5,061,049 (1991).

⁹J. A. Pelesko, in *Nanotech 2001: Technical Proceedings of the 2001 International Conference on Modeling and Simulation of*

- Microsystems*, Vol. 1, p. 290 (NSTI, CA, 2001).
- ¹⁰E. Buks and M. L. Roukes, *Europhys. Lett.* **54**, 220 (2001).
- ¹¹M. Dequesnes, S. V. Rotkin, and N. R. Aluru, *Nanotechnology* **13**, 120 (2002).
- ¹²S. V. Rotkin, *Proc.-Electrochem. Soc.* **6**, 90 (2002).
- ¹³W. H. Lin and Y.-P. Zhao, *Chin. Phys. Lett.* **20**, 2070 (2003).
- ¹⁴R. Seydel, *Practical Bifurcation and Stability Analysis: From Equilibrium to Chaos*, 2nd ed., *Interdisciplinary Applied Mathematics* Vol. 5 (Springer-Verlag, Berlin, 1994).
- ¹⁵W. H. Lin and Y.-P. Zhao, *Chaos, Solitons Fractals* **23**, 1777 (2005).
- ¹⁶H. B. G. Casimir, *Proc. K. Ned. Akad. Wet.* **51**, 793 (1948).
- ¹⁷J. N. Israelachvili, *Intermolecular and Surface Forces* (Academic, London, 1992).
- ¹⁸M. Kardar and R. Golestanian, *Rev. Mod. Phys.* **71**, 1233 (1999).
- ¹⁹P. Meakin, *Phys. Rep.* **235**, 1991 (1994); J. Krim and G. Palasantzas, *Int. J. Mod. Phys. B* **9**, 599 (1995).
- ²⁰C. Genet, A. Lambrecht, P. Maia Neto, and S. Reynaud, *Europhys. Lett.* **62**, 484 (2003); T. Emig, A. Hanke, R. Golestanian, and M. Kardar, *Phys. Rev. Lett.* **87**, 260402 (2001); G. Palasantzas, *J. Appl. Phys.* **97**, 126104 (2005).
- ²¹B. N. J. Persson and E. Tosatti, *J. Chem. Phys.* **115**, 3840 (2001).
- ²²G. Palasantzas, *Phys. Rev. E* **56**, 1254 (1997).
- ²³G. Palasantzas, *Phys. Rev. B* **48**, 14472 (1993); **49**, 5785 (1994).
- ²⁴S. K. Sinha, E. B. Sirota, S. Garoff, and H. B. Stanley, *Phys. Rev. B* **38**, 2297 (1988); H. N. Yang and T. M. Lu, *ibid.* **51**, 2479 (1995); Y. P. Zhao, G. C. Wang, and T. M. Lu, *ibid.* **55**, 13938 (1997).
- ²⁵Y.-P. Zhao, G.-C. Wang, and T.-M. Lu, *Characterization of Amorphous and Crystalline Rough Surfaces: Principles and Applications*, *Experimental Methods in the Physical Science* Vol. 37 (Academic Press, New York, 2001).
- ²⁶R. Esquivel-Sirvent and V. B. Svetovoy, *Phys. Rev. B* **72**, 045443 (2005).
- ²⁷P. A. Maia Neto, A. Lambrecht, and S. Reynaud, *Europhys. Lett.* **69**, 924 (2005); Paulo A. Maia Neto, A. Lambrecht, and S. Reynaud, *Phys. Rev. A* **72**, 012115 (2005).